JACS
JOURNAL OF THE AMERICAN CHEMICAL SOCIETY

Article

pubs.acs.org/JACS

# Electrocatalytic Conversion of Carbon Dioxide to Methane and Methanol on Transition Metal Surfaces

Kendra P. Kuhl, Toru Hatsukade, Etosha R. Cave, David N. Abram, Jakob Kibsgaard, and Thomas F. Jaramillo*

Department of Chemical Engineering, Stanford University, Stanford, California 94305, United States

Supporting Information

**ABSTRACT:** Fuels and industrial chemicals that are conventionally derived from fossil resources could potentially be produced in a renewable, sustainable manner by an electrochemical process that operates at room temperature and atmospheric pressure, using only water, $CO_2$, and electricity as inputs. To enable this technology, improved catalysts must be developed. Herein, we report trends in the electrocatalytic conversion of $CO_2$ on a broad group of seven transition metal surfaces: Au, Ag, Zn, Cu, Ni, Pt, and Fe. Contrary to conventional knowledge in the field, all metals studied are capable of producing methane or methanol. We quantify reaction rates for these two products and describe catalyst activity and selectivity in the framework of CO binding energies for the different metals. While selectivity toward methane or methanol is low for most of these metals, the fact that they are all capable of producing these products, even at a low rate, is important new knowledge. This study reveals a richer surface chemistry for transition metals than previously known and provides new insights to guide the development of improved $CO_2$ conversion catalysts.

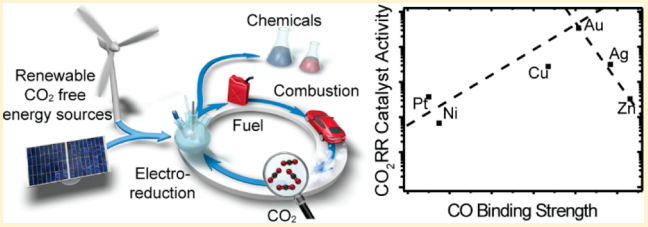


## INTRODUCTION

The modern global energy economy and chemical industry are heavily dependent on fossil resources, but sustainable alternatives need to be developed to secure long-term economic growth while mitigating socio-environmental problems potentially associated with increasing anthropogenic emissions of $CO_2$.[1,2] Incorporation of renewable electricity from wind and solar into the global energy supply is one promising avenue; however, electricity storage is costly for these intermittent resources.[3] One potential solution to alleviate this concern while simultaneously addressing rising concentrations of atmospheric $CO_2$ is the electrochemical reduction of carbon dioxide to carbon-based products.[1,4] With renewable electricity as an input, carbon dioxide and water could be converted in a sustainable fashion into fuels and industrial chemicals, for example, hydrocarbons and alcohols (Figure 1a). Such a process allows energy from an intermittent renewable source to be consumed immediately and in a manner that provides the same types of chemical compounds for which there already exists global-scale demand and infrastructure. Figure 1b shows the half reactions and reduction potentials of several possible $CO_2$ reduction reactions ($CO_2$RRs) along with that of the hydrogen evolution reaction (HER).

A cost-effective process for the electrochemical conversion of carbon dioxide to value-added products requires electrocatalysts that are efficient, selective, and stable. To date, no known catalyst meets these criteria; the development of new catalysts is needed, and to do so, deeper insights into the reaction chemistry are required. Toward this goal, a variety of materials and promoters have previously been examined for $CO_2$RR catalysis, including ionic liquids,[5,6] proteins,[7] organometallic complexes,[8,9] organic compounds,[10] and semiconductors.[11] The majority of studies have focused on transition metals,[11−14] sparked by a 1985 report from Hori and Suzuki that showed methane ($CH_4$) and ethylene ($C_2H_4$) as the main products of the $CO_2$RR on a copper electrode.[15] Several reports since have compared the activity of different transition metals and have found that the product yield and composition of the $CO_2$RR depend on the transition metal's binding energy of CO, believed to be an important intermediate in the reduction of $CO_2$.[16] Metals that bind CO strongly produce few $CO_2$RR products because they are poisoned by CO or other intermediates that form during $CO_2$RR, and consequently, hydrogen ($H_2$), evolved from the competing water reduction, is the main product observed. On the other hand, metals that bind CO weakly produce mostly CO, as the CO is released from the surface before it can be further reduced to products such as alcohols and hydrocarbons. Cu possesses an intermediate binding energy for CO, which is believed to be the reason for its ability to catalyze the formation of more reduced products that require more than a two-electron reduction.[17−19]

In this study, we focus on six transition metals in addition to copper, presenting new results on Au, Ag, and Zn, which bind CO weakly, and Ni, Pt, and Fe, which bind CO strongly (Table

**Received:** June 9, 2014
**Published:** September 26, 2014

   dx.doi.org/10.1021/ja505791r | J. Am. Chem. Soc. 2014, 136, 14107−14113

a

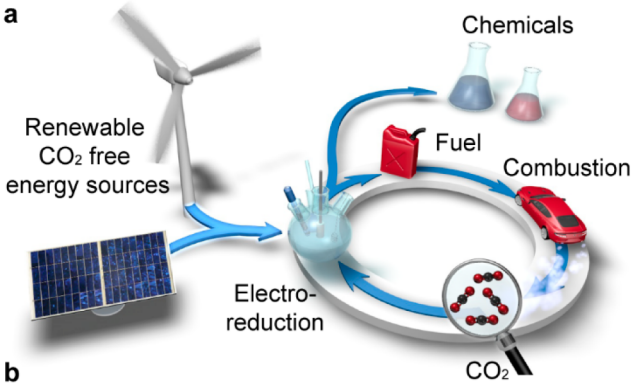


b

| $CO_2$ Reduction Half Reactions | | [V] vs RHE |
|---|---|---|
| $CO_2 + H_2O + 2e^-$ | → $CO + 2OH^-$ | -0.10 |
| $CO_2 + H_2O + 2e^-$ | → $HCOO^- + OH^-$ | -0.03 |
| $CO_2 + 5H_2O + 6e^-$ | → $CH_3OH + 6OH^-$ | 0.03 |
| $CO_2 + 6H_2O + 8e^-$ | → $CH_4 + 8OH^-$ | 0.17 |
| $2CO_2 + 8H_2O + 12e^-$ | → $C_2H_4 + 12OH^-$ | 0.08 |
| $H_2O$ Reduction Half Reaction | | |
| $2H_2O + 2e^-$ | → $2H_2 + 2OH^-$ | 0.0 |

**Figure 1.** Electrochemical reduction of $CO_2$ coupled to renewable electricity sources, such as wind or solar, can potentially enable a $CO_2$-neutral energy cycle in which $CO_2$ is converted to fuels and industrial chemicals in a renewable and sustainable manner.

S1 of the Supporting Information), among the many transition metals worthy of deeper exploration. Utilizing new experimental methods that we have developed,[20] we were able to gather the most consistent data on each metal shown to date. A critical discovery was made during the course of this study: we observed that every one of the seven transition metals examined has the ability to produce either methane or methanol, or both. This is a new insight previously unreported. Furthermore, for metals that can produce both methane and methanol, we find a strong correlation in their rates of production, suggesting commonalities in their mechanistic pathways. In addition, we find that the overall $CO_2$RR activities of the metals studied follow a volcano relationship with respect to their binding energies for CO, with the ideal value near that of Au. Selectivity is another matter, as we find that in order to facilitate the formation of products that require greater than two electrons, for example, methane and methanol, a stronger binding energy for CO is needed. A deeper understanding of the mechanism of methane and methanol formation and associated correlations between the two products, as well as their relationship to CO binding affinity, will help guide the design of improved $CO_2$RR catalysts.

## EXPERIMENTAL SECTION

Experimental methods used in this study have been outlined previously.[20] Briefly, using a custom electrochemical cell, electrolysis experiments were carried out in 0.1 M $KHCO_3$ electrolyte at constant voltage with IR-correction performed by the potentiostat. Gas chromatography was used to quantify the amount of gas-phase products, and NMR was used to quantify the concentration of liquid-phase products. From the concentrations, it was possible to calculate current efficiencies and partial current densities for each product. Multiple electrolysis experiments were run at each potential, and the results were averaged to give the data reported herein. Deionized water from a Millipore system (18.2 MΩ·cm) was used throughout.

Cu. The foil was purchased from Alfa Aesar (1.0 mm thick, product #42975, 99.999% metals basis). Before each electrolysis experiment, the foil was mechanically polished (400G sandpaper, 3M) and then was electrochemically polished at 2.1 V versus a graphite foil counter electrode in 85% $H_3PO_4$ followed by rinsing with water.

Ni. The foil was purchased from Alfa Aesar (0.1 mm thick, product #12046, lot #B11X051 and G29U009, 99.994% metals basis). Before each electrolysis experiment, the foil was mechanically polished (400G sandpaper, 3M) and was rinsed with water.

Fe. The foil was purchased from Alfa Aesar (0.1 mm thick, product #40493, lot #B27U015, 99.99% metals basis). Before each electrolysis experiment, the foil was mechanically polished (400G sandpaper, 3M) and was rinsed with water.

Pt. The foil was purchased from Alfa Aesar (0.05 mm thick, product #42456, lot #J19R006, 99.99% metals basis). Before each electrolysis experiment, the foil was electrochemically cleaned by applying +4 V versus a Pt mesh in 30% nitric acid and by rinsing with water, and the PtO surface was potentiostatically reduced at −0.20 V versus Ag/AgCl for 3 min in the electrolysis cell immediately prior to electrolysis.

Zn. The foil was purchased from Alfa Aesar (1.0 mm thick, product #11915, lot #J08S021, 99.9985% metals basis). Before each electrolysis experiment, the foil was mechanically polished (400G sandpaper, 3M) and was rinsed with water.

Ag. The foil was purchased from Alfa Aesar (0.1 mm thick, product #12126, lot #D22W016, 99.998% metals basis). Before each electrolysis experiment, the foil was mechanically polished (400G sandpaper, 3M) and was rinsed with water.

Au. The foil was purchased from Alfa Aesar (0.1 mm thick, product #11391, lot #C01Y014, 99.9975+% metals basis). Au foils were left overnight in concentrated nitric acid and were rinsed with water prior to each experiment. Au foils were also held at 2.3 V versus RHE (reversible hydrogen electrode) for 30 min prior to the start of $CO_2$ electroreduction; similar results on Au were observed for samples that did not undergo the anodic hold.

## RESULTS AND DISCUSSION

For each metal studied, potentiostatic electrolysis experiments were conducted over a range of potentials; the average current density is shown in Figure 2a. The products of $CO_2$RR in the gas phase and in the liquid phase and the amount of hydrogen formed by competing water reduction were measured at each potential. Figure 2b shows the percentage of the total current at each potential that goes toward $CO_2$RR instead of making hydrogen. This data confirms what has been reported previously: Au, Ag, and Zn, which bind CO weakly, exhibit a high current efficiency for $CO_2$ reduction whereas Ni, Pt, and Fe, which bind CO strongly, are poor $CO_2$ reduction catalysts as they mostly produce hydrogen. Cu, with a moderately strong CO binding energy, shows a high current efficiency for $CO_2$RR but less than that of Au, Ag, or Zn. Our measurements as a function of potential reveal that the current efficiency for $CO_2$RR on Au, Ag, Zn, and Cu generally increases as overpotential increases, until reaching a peak after which the current efficiency decreases. The decrease in $CO_2$RR current efficiency at high overpotentials could result from $CO_2$ mass transport limitations or could indicate that the $CO_2$RR is


dx.doi.org/10.1021/ja505791r | J. Am. Chem. Soc. 2014, 136, 14107−14113

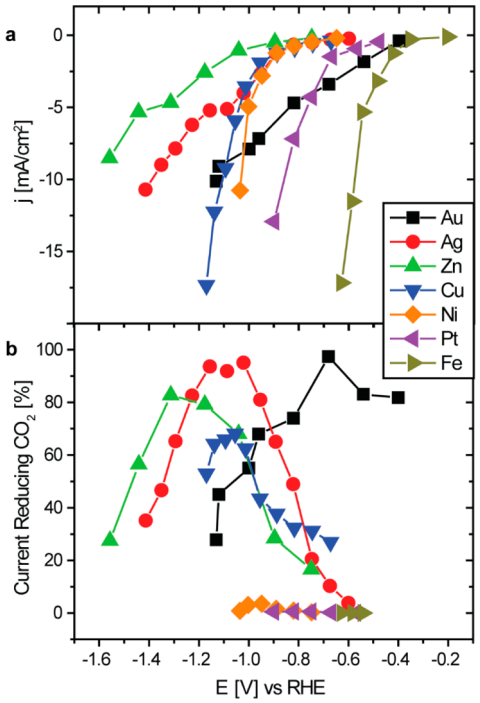


**Figure 2.** (a) Current densities during 1 h long potentiostatic $CO_2$ electrolysis experiments. (b) Current efficiencies (%) for the $CO_2$ reduction reaction ($CO_2$RR) at each potential.

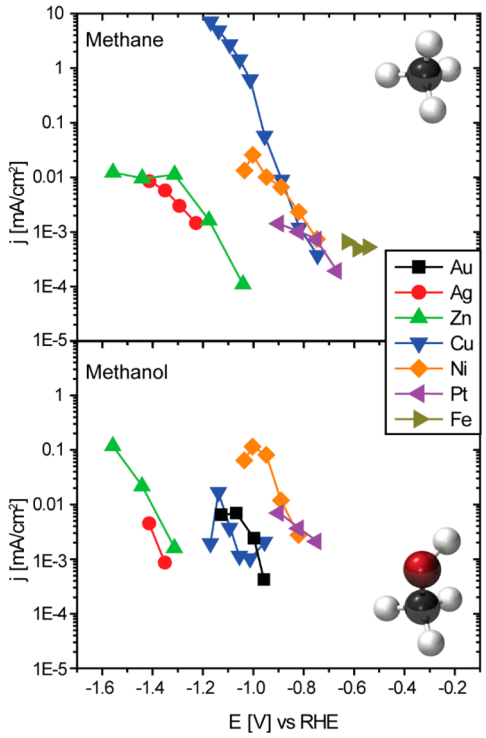


**Figure 3.** Partial current densities of methane and methanol.

outcompeted by hydrogen evolution at such negative potentials (see Supporting Information for further discussion).

While Figure 2 shows important activity trends for the transition metals studied, a deeper understanding may be gained by examining the product distribution, that is, selectivity, in greater detail over the potential range. Using our methods, sensitive to the identification and quantification of reaction products, here we report several new products for these metal surfaces. In particular, we found that Cu is not unique in the ability to catalyze hydrocarbon and alcohol formation. All of the metals tested in this study produced methane, methanol, or both, along with several other minor products. To rule out the possibility that liquid-phase products observed in this study come from sources other than $CO_2$ reduction, for example, carbonaceous contamination,[21,22] isotope-labeled $^{13}CO_2$ was used to study the $^{13}CO_2$RR on each metal at a potential where novel minor products were observed. The incorporation of the $^{13}C$ label into the products was confirmed by the peak splitting observed in $^{1}H$ NMR; see Figure S2 of the Supporting Information.

Table S2 of the Supporting Information compares previous literature reports to the data collected in this study. The main difference between the data sets is that we observe alcohols or hydrocarbons with all the metal catalysts tested. This can be partially explained by the sensitivity of our methods for product detection. In many cases, however, the potential where we first detected the formation of more reduced products was more negative than the potential explored in previous reports. This also highlights the importance of studying catalysts over a wide potential range in order to gain important insights into activity.

While all the metals tested could produce methane or methanol, most produced both. Au and Fe are the two exceptions, producing only methanol and methane, respectively, within the potential range tested. Figure 3 shows the partial current densities for methane and methanol as a function of applied potential for each of the seven metals; partial current density is a measure of reaction rate that scales linearly with turnover frequency (TOF). Among the seven metals, there is a wide variation in onset potentials for methane and methanol, defined for the purposes of this discussion as the earliest potential at which the reaction product is observed by our analytical methods. For instance, Fe exhibits the earliest onset for any product that requires greater than two electrons, producing methane at −0.53 V versus RHE, whereas Ag requires a voltage of −1.22 V versus RHE to produce methane and a voltage of −1.35 V versus RHE to produce methanol.

Interestingly, for each of the five metals that can produce both methane and methanol, only a small difference in onset potential is observed between the two products for that particular surface. Generally, methane emerges at lower potentials by a small margin, which could be explained in part by our experimental methods' somewhat greater sensitivity to methane than to methanol.[20] Figure 3 also shows that the partial current densities of methane and methanol generally correlate with one another on each metal surface. These observations suggest commonalities in their mechanistic pathways. For instance, each product could have a rate-determining step (rds) in the reaction sequence that is similarly difficult to surmount; after the rds, both products are thermodynamically downhill. It is also plausible that methane and methanol may share several common intermediates. To produce methanol, a catalyst needs to break just one C−O bond in $CO_2$, while to produce methane, both C−O bonds must be broken. If a catalyst breaks both C−O bonds early in the reaction, producing an oxygenated product such as methanol would not be expected at these reducing potentials; methane would be the only plausible C1 product. However, as most metals in this study were found to catalyze the formation of both methane and methanol, with the product formation


dx.doi.org/10.1021/ja505791r | J. Am. Chem. Soc. 2014, 136, 14107−14113

rates generally tracking one another across the potential range, it follows that the second C−O bond cleavage step that leads to methane likely occurs later in the reaction pathway.

The favorability of cleaving of the final C−O bond could explain the product selectivity observed for Fe and Au, with Fe favoring methane with no methanol detected and vice versa for Au. Interestingly, Fe and Au lie at the strong and weak extremes of oxygen-binding energies, respectively (Table S1 of the Supporting Information). With this in mind, the Fe surface could favor breaking the second C−O bond early in the reaction as Fe exhibits a strong binding affinity for oxygen (Table S1 of the Supporting Information). In fact, ultrahigh vacuum (UHV) experiments of CO on Fe surfaces have shown that CO dissociates to adsorbed $C_{ads}$ and $O_{ads}$, even at low temperatures, because of its high oxophilicity.[23,24] If Fe breaks both C−O bonds early in the reaction sequence, it may explain why methane is observed as a product but not methanol. Au, on the other hand, exhibits a very weak affinity for oxygen (Table S1 of the Supporting Information) which may favor leaving the C−O bond intact, leading to methanol instead of methane. The selectivity of Fe for hydrocarbons instead of alcohols at a low overpotential suggests that hydrocarbon production could be improved by engineering a surface that binds $O_{ads}$ and $C_{ads}$ strongly, which would facilitate C−O bond dissociation, but that has a weak binding energy for $H_{ads}$, so that HER is disfavored. The oxygen-binding energies of the other five metal surfaces are all in-between those of Au and Fe, which could explain, in part, why those metals produce measurable amounts of both methane and methanol rather than just one or the other.

Given the importance of CO as a reactive intermediate in the $CO_2RR$,[19,25] to better understand the behavior of these catalysts, we construct Figure 4 in which a plot of the $CO_2RR$ activity and selectivity data from Figures 2 and 3 against the density functional theory (DFT) calculated binding energy of CO onto step sites for each metal surface (Table S1 of the Supporting Information).[26,27] A vertical line labeled CO*|CO(g) is included in Figure 4 for reference to indicate the thermodynamics of chemical CO adsorption/desorption;[19] metal surfaces that favor CO in an adsorbed state, CO*, are located to the left of the line while those that favor CO desorption, CO(g), are located to the right. Figure 4 is presented as a framework for understanding activity and selectivity for different $CO_2RR$ products on the basis of CO binding energy as a descriptor for the reaction.

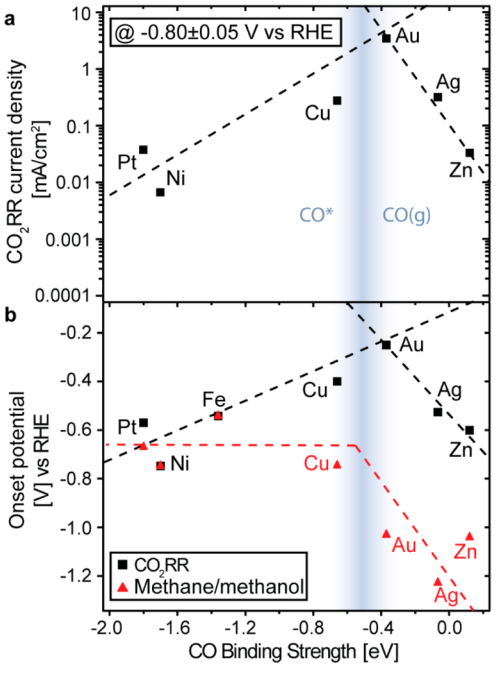


**Figure 4.** (a) Volcano plot of partial current density for $CO_2RR$ at −0.8 V vs CO binding strength. (b) Three distinct onset potentials plotted vs CO binding energy: the HER, the overall $CO_2RR$, and methane or methanol. Dashed lines are to guide the eye.

A useful figure of merit to compare $CO_2RR$ activity among catalysts is by means of their partial current density for the $CO_2RR$ (to any product) at a common potential. Given the vastly different current−voltage profiles of Figure 2, there was no common potential for which $CO_2RR$ activity could be measured on all seven metals. Measurements on six of the seven metals (Pt, Ni, Cu, Au, Ag, Zn), however, could be obtained at a common potential, −0.80 ± 0.05 V versus RHE. Figure 4a shows this data, plotting the partial current densities for the $CO_2RR$ at this potential versus CO binding energy, where a volcano-shaped trend emerges. As seen in Figure 4a, Au has the highest partial current density for the $CO_2RR$ and thus represents the peak of the plot with activity decreasing for metals on either side. The volcano-shaped activity trend for $CO_2RR$ has been explained previously by DFT calculations[19] that suggest that metals with a lower CO binding energy than Au, such as Ag and Zn, exhibit lower activity than Au for the $CO_2RR$ because of slower activation of $CO_2$, the first step in the $CO_2RR$ reaction sequence. Conversely, metals that bind CO more tightly, namely Cu, Ni, Pt, and Fe, while effective at activating $CO_2$ are limited by slow CO desorption or further reaction of CO to other products because of the strong surface−CO bond.[28−31] Thus, overall $CO_2RR$ activity is observed when CO can desorb from the surface or when overpotentials are reached that can continue to reduce adsorbed CO to other products that can emerge from the surface, for example, methane or methanol.

In considering overall $CO_2RR$ activity (converting $CO_2$ to any product), the data in Figure 4a suggest that Au has a CO binding energy closer to the ideal value than any of the other metals investigated in this study. However, selectivity is also an important concern. The major product of $CO_2RR$ on Au is CO, whereas Cu, located on the strong-binding side of Au, exhibits greater selectivity toward more reduced products that can readily serve as fuels or industrial chemicals, for example, hydrocarbons and alcohols.[20] This suggests that to favor such $CO_2RR$ products with greater than two electrons transferred, catalyst surfaces with CO binding energies stronger than that of Au are desirable.

To explore selectivity further, we examined onset potential as another important figure of merit that can describe catalytic activity and selectivity. For each of the seven metals investigated, Figure 4b plots two different $CO_2RR$ onset potentials with respect to CO binding energy: one for the overall $CO_2RR$ (i.e., for the first $CO_2RR$ product to be detected) and one for the specific $CO_2RR$ products of methane or methanol (denoted as methane/methanol). Many trends in onset potential are apparent. First, one can observe an overall $CO_2RR$ activity volcano that is similar in shape to that presented in Figure 4a above it, again with Au near the peak. The fact that the same trend in overall $CO_2RR$ activity is observed in Figure 4b as in Figure 4a, with the two plots using


dx.doi.org/10.1021/ja505791r | J. Am. Chem. Soc. 2014, 136, 14107−14113

completely distinct experimentally derived figures of merit for $CO_2RR$ catalysis, further emphasizes the relevance of this type of relationship between overall $CO_2RR$ activity and CO binding energy.

The methane/methanol onset potentials plotted in Figure 4b, however, reveal very different behavior with respect to CO binding energy compared to that for the overall $CO_2RR$. The broad range of metals can be classified in two distinct regimes: metals that bind CO weakly (Au, Ag, and Zn) located to the right of the CO*|CO(g) line and the metals on the left that bind CO more tightly (Cu, Ni, Pt, and Fe). The first observation to note is that metals on the right exhibit much later onset potentials for methane/methanol than the metals on the left of the CO*|CO(g) line. A second observation is that the metals on the left, the strong CO-binding side, all exhibit fairly similar onset potentials for methane/methanol irrespective of their particular value of CO binding energy, as indicated by the effectively flat trend line drawn to guide the eye. The distinct behavior observed across the two regimes of CO binding can be explained by two crucial phenomena: (1) The ability for each metal to reduce adsorbed CO and (2) the coverage of CO on each surface under $CO_2RR$ conditions.

There is spectroscopic evidence to suggest that during $CO_2$ reduction there is a high surface coverage of adsorbed CO on Cu,[25,32] Ni,[28,29] Pt,[33] and Fe.[29] High CO coverage on these metals could imply that the reduction of adsorbed CO is the rate-determining step to produce desirable reduced products such as methane/methanol, a view that has been supported by recent theory.[19,34] DFT calculations have also suggested that for metal surfaces, the thermochemistry of the reaction step in which adsorbed CO is reduced is rather insensitive with respect to CO binding energy.[19] Hence, a flat trend line in methane/methanol onset potentials would be expected for metals operating at fairly high CO coverage across a wide range of CO binding energies, which is exactly what is observed experimentally for all metals to the left of the CO*|CO(g) line in Figure 4b, with onset potentials of approximately −0.65 V ± 0.1 V versus RHE. These are fairly negative potentials for all metals.

As mentioned earlier and shown in Figure 4b, the ability to catalyze the production of methane/methanol is quite different for metals that bind CO weakly, namely, Au, Ag, and Zn. The arguments above, where the thermochemistry of reducing adsorbed CO is fairly insensitive to CO binding energy, would imply that the weak CO binding metals would also be expected to be as proficient in executing this step as metals that bind CO strongly. However, another important factor plays a role: For metals that bind CO weakly, CO reduction competes against the very kinetically fast process of CO desorption. Once $CO_2$ is converted to adsorbed CO on these metals, the CO readily desorbs before it could be further reduced to alcohol or hydrocarbon products. This explains the large difference observed, approximately 0.3−0.6 V, in the measured onset potential for the overall $CO_2RR$ (where CO is the first product) versus that for methane/methanol; only at extremely high overpotentials can the rate of CO reduction begin to compete with the fast rate of CO desorption, consistent with overpotentials in the range of 1.0−1.2 V needed to produce methane/methanol at a measurable rate for the weak CO binding metals.

While Figure 4 plots activity and selectivity data versus CO binding energies calculated for stepped sites, we note that the analysis is robust with respect to other types of surface sites expected on the polycrystalline metals investigated in this study. For the sake of comparison, Table S1 of the Supporting Information also shows DFT-calculated CO binding energies for other possible surface sites in addition to experimentally derived values for CO binding energy. There is general agreement in the trends for CO-binding, whether using values from theory or experiment, or among different types of surface sites, which facilitates analysis. Figure S4 of the Supporting Information plots the $CO_2RR$ activity and selectivity data against these additional CO binding values and shows identical trends as those observed in Figure 4; thus, the same conclusions can be drawn irrespective of the particular surface site, further supporting the relevance of CO binding energy as a descriptor for the $CO_2RR$.

No discussion of $CO_2RR$ kinetics is complete without addressing the HER, as $H_2$ production is undesirable when $CO_2RR$ products are the target. HER is widely regarded as a more kinetically facile reaction that can compete against $CO_2RR$, decreasing $CO_2RR$ selectivity.[19] For all seven metals, $H_2$ is observed as a product either simultaneously with, or even before, any $CO_2RR$ products. Interestingly, among the seven metals examined, we find that Pt, generally considered the most active HER catalyst,[35] is not the most active for the HER under $CO_2RR$ conditions. Fe clearly exhibits the highest HER current density at any given applied potential (Figure 2a), despite the fact that Fe is not known to be particularly active for the HER under more conventional conditions.[35] This major change in the ranking of activities among HER catalysts when examined under $CO_2RR$ conditions suggests the surface chemistry of adsorbed species is indeed complex, with coverage effects and adsorbate−adsorbate interactions potentially playing significant roles.[36]

## ■ CONCLUSIONS

In this report, we investigate the activity and selectivity for the $CO_2$ reduction reaction ($CO_2RR$) among seven transition metal surfaces: Au, Ag, Zn, Cu, Ni, Pt, and Fe. Bringing to bear new experimental methods with unprecedented sensitivity to identify and quantify reaction products, we have provided new insights into $CO_2$ reaction chemistry. Adding important new knowledge to the field, we have found that all of these transition metals are capable of producing methane or methanol, with at least five of the metals (Zn, Ag, Cu, Ni, and Pt) able to produce both. Quantitative measurements of the partial current density of these two products as a function of applied potential revealed a close correlation in their reaction rates. This allowed us to conclude that methane and methanol share commonalities in their mechanisms. More generally, it was found that many of the trends observed in activity and selectivity for $CO_2RR$ products, and particularly for methane and methanol, can be explained at least in part by each surface's binding energy for CO. Our results confirm the importance of this reaction intermediate and provide greater insight as to how the CO binding energy impacts catalyst behavior. Ongoing work exploring the activity of transition metals for the reduction of CO, formate, and other small organic molecules will further increase our understanding of the roles of important intermediates and activity trends in the $CO_2RR$.

We also find that the oxophilicity of the surface, as determined by binding energy of $O_{ads}$, could play an important role in the reaction, in particular for determining selectivity between methane and methanol. We detect no methane but only methanol on Au, the least oxophilic metal of the group of

seven, whereas for Fe, the most oxophilic of the group, we detect methane but not methanol. This provides key insights as to how one might engineer a surface to improve selectivity toward one product or the other by modifying the binding energy for $C_{ads}$ and $O_{ads}$ to favor or disfavor C−O bond breakage. Controlling the $H_{ads}$ binding energy will also be key for disfavoring competing HER. These adsorbate binding characteristics are particularly important to investigate under the reaction conditions relevant to the $CO_2$RR.

The results of this study offer the most consistent and complete picture available to date regarding the $CO_2$RR activity and selectivity for these elemental transition metal catalysts. The insights gained demonstrate the importance of measuring $CO_2$RR activity over a wide range of potentials with methods capable of identifying and quantifying even minor products. Our findings show that the surface chemistry of elemental transition metals is richer than previously thought and that electrocatalysts that can produce hydrocarbons or alcohols are not as elusive as previously believed. The deeper understanding of transition-metal catalysts presented here provides important guidance in searching for catalysts with higher $CO_2$RR activity and selectivity by means of tuning adsorbate binding energies appropriately, perhaps in the form of transition-metal alloys. Improved $CO_2$RR catalysts could enable new technologies with the ability to address the intermittent nature of renewable electricity while recycling $CO_2$ to produce fuels and industrial chemicals that carry global importance in a sustainable manner, free of fossil fuels.

## ■ ASSOCIATED CONTENT

### Supporting Information

Binding strength of CO and O, mass transport limitations, minor products of $CO_2$RR, isotope-labeled $^{13}CO_2$ reduction, trace metal impurities, additional volcano plots. This material is available free of charge via the Internet at http://pubs.acs.org.

## ■ AUTHOR INFORMATION


### Corresponding Author

jaramillo@stanford.edu


### Author Contributions

The manuscript was written through contributions of all authors.

### Notes

The authors declare no competing financial interest.

## ■ ACKNOWLEDGMENTS

This material is based upon work supported by the National Science Foundation under Grant Number 1066515 and by the Global Climate & Energy Project (GCEP) at Stanford University. T.F.J. gratefully acknowledges partial support provided by the MDV Innovator Award program at Mohr Davidow Ventures. K.P.K. and E.R.C. acknowledge support by the National Science Foundation Graduate Research Fellowship under Grant No. (DGE-1147470). E.R.C. acknowledges support from the Ford Foundation. D.N.A. acknowledges support from a Stanford Graduate Fellowship. The authors would like to thank Dr. Corey Liu of the Stanford Magnetic Resonance Laboratory and Dr. Stephen R. Lynch of the Stanford Chemistry for technical assistance with NMR experiments. The authors would also like to thank Dr. Zhebo Chen, Dr. Arnold Forman, Prof. Andrew A. Peterson, Prof. Anders Nilsson and Prof. Jens K. Nørskov for helpful discussions.

## ■ REFERENCES


(1) Lewis, N. S.; Nocera, D. G. *Proc. Natl. Acad. Sci. U.S.A.* **2006**, *103*, 15729.
(2) Olah, G. A.; Prakash, G. K. S.; Goeppert, A. *J. Am. Chem. Soc.* **2011**, *133*, 12881.
(3) Barnhart, C. J.; Benson, S. M. *Energy Environ. Sci.* **2013**, *6*, 1083.
(4) Gattrell, M.; Gupta, N.; Co, A. *Energy Convers. Manage* **2007**, *48*, 1255.
(5) Lin, J.; Ding, Z.; Hou, Y.; Wang, X. *Sci. Rep.* **2013**, *3*, DOI: 10.1038/srep01056.
(6) Rosen, B. A.; Salehi-Khojin, A.; Thorson, M. R.; Zhu, W.; Whipple, D. T.; Kenis, P. J. A.; Masel, R. I. *Science* **2011**, *334*, 643.
(7) Woolerton, T. W.; Sheard, S.; Reisner, E.; Pierce, E.; Ragsdale, S. W.; Armstrong, F. A. *J. Am. Chem. Soc.* **2010**, *132*, 2132.
(8) Hull, J. F.; Himeda, Y.; Wang, W.-H.; Hashiguchi, B.; Periana, R.; Szalda, D. J.; Muckerman, J. T.; Fujita, E. *Nat. Chem.* **2012**, *4*, 383.
(9) Angamuthu, R.; Byers, P.; Lutz, M.; Spek, A. L.; Bouwman, E. *Science* **2010**, *327*, 313.
(10) Cole, E. B.; Lakkaraju, P. S.; Rampulla, D. M.; Morris, A. J.; Abelev, E.; Bocarsly, A. B. *J. Am. Chem. Soc.* **2010**, *132*, 11539.
(11) Dhakshinamoorthy, A.; Navalon, S.; Corma, A.; Garcia, H. *Energy Environ. Sci.* **2012**, *5*, 9217.
(12) Salehi-Khojin, A.; Jhong, H.-R. M.; Rosen, B. A.; Zhu, W.; Ma, S.; Kenis, P. J. A.; Masel, R. I. *J. Phys. Chem. C* **2012**, *117*, 1627.
(13) Schouten, K. J. P.; Kwon, Y.; van der Ham, C. J. M.; Qin, Z.; Koper, M. T. M. *Chem. Sci.* **2011**, *2*, 1902.
(14) Chen, Y.; Li, C. W.; Kanan, M. W. *J. Am. Chem. Soc.* **2012**, *134*, 19969.
(15) Hori, Y.; Kikuchi, K.; Suzuki, S. *Chem. Lett.* **1985**, 1695.
(16) Gattrell, M.; Gupta, N.; Co, A. *J. Electroanal. Chem.* **2006**, *594*, 1.
(17) *Handbook of Fuel Cells: Fundamentals, Technology and Application*; Hori, Y., Ed.; VHC-Wiley: Chichester, U.K., 2003; Vol. *2*.
(18) Peterson, A. A.; Abild-Pedersen, F.; Studt, F.; Rossmeisl, J.; Norskov, J. K. *Energy Environ. Sci.* **2010**, *3*, 1311.
(19) Peterson, A. A.; Norskov, J. K. *J. Phys. Chem. Lett.* **2012**, *3*, 251.
(20) Kuhl, K. P.; Cave, E. R.; Abram, D. N.; Jaramillo, T. F. *Energy Environ. Sci.* **2012**, *5*, 7050.
(21) Yang, C.-C.; Yu, Y.-H.; van der Linden, B.; Wu, J. C. S.; Mul, G. *J. Am. Chem. Soc.* **2010**, *132*, 8398.
(22) Yui, T.; Kan, A.; Saitoh, C.; Koike, K.; Ibusuki, T.; Ishitani, O. *ACS Appl. Mater. Interfaces* **2011**, *3*, 2594.
(23) Gonzalez, L.; Miranda, R.; Ferrer, S. *Surf. Sci.* **1982**, *119*, 61.
(24) Seip, U.; Tsai, M. C.; Christmann, K.; Kuppers, J.; Ertl, G. *Surf. Sci.* **1984**, *139*, 29.
(25) Hori, Y.; Murata, A.; Yoshinami, Y. *J. Chem. Soc., Faraday Trans.* **1991**, *87*, 125.
(26) Jiang, T.; Mowbray, D. J.; Dobrin, S.; Falsig, H.; Hvolbæk, B.; Bligaard, T.; Nørskov, J. K. *J. Phys. Chem. C* **2009**, *113*, 10548.
(27) Hummelshøj, J. S.; Abild-Pedersen, F.; Studt, F.; Bligaard, T.; Nørskov, J. K. *Angew. Chem., Int. Ed.* **2012**, *51*, 272.
(28) Hori, Y.; Koga, O.; Aramata, A.; Enyo, M. *Bull. Chem. Soc. Jpn.* **1992**, *65*, 3008.
(29) Koga, O.; Matsuo, T.; Yamazaki, H.; Hori, Y. *Bull. Chem. Soc. Jpn.* **1998**, *71*, 315.
(30) Hori, Y.; Takahashi, R.; Yoshinami, Y.; Murata, A. *J. Phys. Chem. B* **1997**, *101*, 7075.
(31) Hansen, H. A.; Varley, J. B.; Peterson, A. A.; Nørskov, J. K. *J. Phys. Chem. Lett.* **2013**, *4*, 388.
(32) Hori, Y.; Wakebe, H.; Tsukamoto, T.; Koga, O. *Surf. Sci.* **1995**, *335*, 258.
(33) Taguchi, S.; Aramata, A.; Enyo, M. *J. Electroanal. Chem.* **1994**, *372*, 161.
(34) Nie, X.; Esopi, M. R.; Janik, M. J.; Asthagiri, A. *Angew. Chem., Int. Ed.* **2013**, *52*, 2459.
(35) Greeley, J.; Markovic, N. M. *Energy Environ. Sci.* **2012**, *5*, 9246.

(36) Shi, C.; Hansen, H. A.; Lausche, A. C.; Norskov, J. K. *Phys. Chem. Chem. Phys.* **2014**, *16*, 4720.